Analysis of the Functional Coupling between Calmodulin's Calcium Binding and Peptide Recognition Properties†

Salida Mirzoeva,‡ Steven Weigand,‡ Thomas J. Lukas, Ludmila Shuvalova, Wayne F. Anderson, and D. Martin Watterson*

Department of Molecular Pharmacology and Biological Chemistry and Drug Discovery Program, Northwestern University, Chicago, Illinois 60611

Received September 2, 1998; Revised Manuscript Received December 28, 1998

ABSTRACT: The enhancement of calmodulin's (CaM) calcium binding activity by an enzyme or a recognition site peptide and its diminution by key point mutations at the protein recognition interface (e.g., E84K-CaM), which is more than 20 Å away from the nearest calcium ligation structure, can be described by an expanded version of the Adair−Klotz equation for multiligand binding. The expanded equation can accurately describe the calcium binding events and their variable linkage to protein recognition events can be extended to other CaM-regulated enzymes and can potentially be applied to a diverse array of ligand binding systems with allosteric regulation of ligand binding, whether by other ligands or protein interaction. The 1.9 Å resolution X-ray crystallographic structure of the complex between E84K-CaM and RS20 peptide, the CaM recognition site peptide from vertebrate smooth muscle and nonmuscle forms of myosin light chain kinase, provides insight into the structural basis of the functional communication between CaM's calcium ligation structures and protein recognition surfaces. The structure reveals that the complex adapts to the effect of the functional mutation by discrete adjustments in the helix that contains E84. This helix is on the amino-terminal side of the helix−loop−helix structural motif that is the first to be occupied in CaM's calcium binding mechanism. The results reported here are consistent with a sequential and cooperative model of CaM's calcium binding activity in which the two globular and flexible central helix domains are functionally linked, and provide insight into how CaM's calcium binding activity and peptide recognition properties are functionally coupled.

Calmodulin (CaM)[1] is the most extensively studied member of a class of proteins used by eukaryotic cells to transduce intracellular calcium signals into biological responses (for a recent review, see ref *1*). CaM serves this biological role through its ability to function as a calcium binding regulatory subunit of a diverse array of enzymes, structural proteins, and membrane transporters. Variations on common molecular themes provide potential mechanisms for the differential response of CaM-regulated pathways to calcium signals (*2*). These include the varied expression of specific CaM-regulated enzymes or isozymes among tissues, differential subcellular localization provided through targeting sequences in the CaM-regulated enzyme, and differential calcium binding affinity of CaM due to its presence in supramolecular complexes with various CaM binding structures. While an increasing level of insight into the molecular basis of differential expression and localization has been provided by the study of CaM-regulated enzymes and their genes, less is known about the coupling of CaM's calcium binding activity to its enzyme regulation and recognition properties. Because CaM-mediated pathways involve a single protein in several discrete biological responses, knowledge about this early step that is common to multiple signal transduction pathways is required for an understanding of how eukaryotic cells integrate their differential responses to environmental stimuli and maintain organismal homeostasis.

The diverse biological, biochemical, and physical methods used in the search for fundamental themes in CaM-mediated calcium signal transduction pathways have revealed conserved features of CaM and related them to cellular function and enzyme regulation (for a recent review in relation to CaM-regulated protein kinases, see ref *2*). For example, phylogenetic analyses have revealed sets of amino acids in CaM that have been conserved for an estimated 1 billion years, and site-directed mutagenesis and functional analyses have demonstrated the importance of such conserved amino acids in enzyme regulatory activity and eukaryotic cell survival (*3*). While a variety of charged and hydrophobic amino acids throughout the CaM sequence exhibit phylogenetic conservation and have been correlated with CaM's biochemical activities (*4*−*13*), E84 is the only single amino acid that has been demonstrated to be critical for both in vitro and in vivo function (*9*−*14*).

† Supported in part by National Institutes of Health Grant GM 30861. D.M.W. is the John G. Searle Professor of Molecular Biology and Biochemistry.

* Corresponding author: 303 E. Chicago Ave., Chicago, IL 60611-3008. Telephone: (312) 503-0656. Fax: (312) 503-1300. E-mail: m-watterson@nwu.edu.

‡ Both authors contributed equally to this project.

[1] Abbreviations: CaM, calmodulin; MLCK, myosin light chain kinase; sm/nmMLCK, smooth muscle/nonmuscle myosin light chain kinase; skMLCK, skeletal muscle myosin light chain kinase; CaMPKII, calmodulin-dependent protein kinase II; DTT, dithiothreitol; HEPES, 4-(2-hydroxyethyl)-1-piperazineethanesulfonic acid; EDTA, ethylenediaminetetraacetic acid; EGTA, ethylene glycol bis(β-aminoethyl ether)-*N*,*N*,*N*′,*N*′-tetraacetic acid; PBS, phosphate-buffered saline; Tris, tris(hydroxymethyl)aminomethane.

10.1021/bi9821263 CCC: $18.00
Published on Web 03/12/1999

Quantitative analyses of the functional importance of phylogenetically conserved amino acids of CaM have benefited from the study of the broadly distributed vertebrate smooth muscle and nonmuscle myosin light chain kinase isozyme (sm/nmMLCK) and its more restricted skeletal muscle isozyme (skMLCK). These are experimentally attractive enzymes that have revealed fundamental themes reiterated in a broad array of CaM-regulated proteins (for recent reviews, see refs *2* and *15*). Briefly, MLCKs were the first enzymes for which a CaM recognition site was identified (*16*, *17*), and are the most thoroughly characterized of the CaM-regulated enzymes (*2*). The segmental organization of function in the primary structure of CaM-regulated enzymes and the relief-of-autoinhibition mechanism of enzyme activation by CaM are two themes that were elucidated through studies of MLCKs (*13*) and have since been found in most CaM-regulated enzymes (*2*). In the case of the sm/nmMLCK, synthetic peptide analogue studies (*17*) and site-directed mutagenesis of the enzyme (*13*) demonstrated that the CaM recognition properties of sm/nmMLCK can be mimicked to a significant extent by more experimentally tractable peptide analogues, called RS20 peptide sequences (*13*, *17*).

The availability of the RS20 peptide analogue and chemically homogeneous mutant sm/nmMLCKs allowed the experimental uncoupling of the enzyme binding step from the enzyme activation step in the molecular mechanism of CaM regulation, and the mechanistic study of complementary features in CaM and a CaM-regulated enzyme. For example, CaMs mutated at the phylogenetically conserved E84 were found to have selectively diminished sm/nmMLCK activator activity (*9*, *13*), and this loss of function could be suppressed by complementary charge reversal mutations of sm/nmMLCK in the CaM recognition segment (*13*). The later determination of the crystallographic structure of a complex between CaM and an RS20 peptide analogue (*18*) demonstrated that E84 of CaM was a contact residue at the interface with the peptide, and provided insight into the structural basis of the recognition between CaM and sm/nmMLCK. On the basis of an array of hydrophobic interactions at the interface between CaM and the peptide, site-directed mutagenesis of specific methionine residues (M71, M72, M109, and M124) of CaM demonstrated (*4*) their importance in the activation of sm/nmMLCK. Therefore, a variety of structural, chemical modification, site-directed mutagenesis, and activity results reported over the past decade are in agreement concerning the importance of the RS20 sequence of sm/nmMLCK in CaM recognition, and the functional importance of key hydrophobic and charged amino acids of CaM found at the peptide recognition interface (*2*).

Although there is general agreement about the biochemical relevance of CaM's interaction with RS20 peptide sequences and the functional importance of certain hydrophobic and charged residues of CaM at the structural interface (*4*, *5*, *13*, *18*), the importance of these key interface amino acids to CaM's calcium binding activity at structurally distant calcium ligation sites has not been addressed. This is especially important in light of the demonstration (*19*) that the RS20 peptide is able to mimic sm/nmMLCK's enhancement of CaM's affinity for calcium, and to suppress the loss of calcium binding activity resulting from mutations of calcium ligation residues in CaM. However, the available crystallographic (*18*) and NMR-based structures (*20*−*22*) for complexes of CaM−RS20 peptide analogues have demonstrated that the nearest calcium ligation site of CaM is distant from the functionally important interface residues. A full understanding of the physiological roles of CaM−enzyme complexes in the integration of intracellular calcium signals requires that we gain additional insights into how the interaction of CaM with specific enzymes is related to CaM's calcium binding activity, and whether the loss of CaM's enzyme activation activity by mutation at interface residues has any effect on CaM's signature calcium binding and calcium-dependent regulatory activities.

While much has been learned over the past decade about CaM's enzyme recognition and ion binding properties, controversy concerning the mechanism of calcium binding still exists. It is now widely accepted that there is an ordered binding of calcium (i.e., the first site to be occupied in the mechanism is the calcium ligation structure III, and then ligation structure IV, followed by binding to the amino-terminal pair of calcium ligation structures), and that there is cooperativity between each pair of sites found in each of the two globular domains (*1*, *19*, *23*, *24*). The controversy surrounds whether CaM is composed of two coupled globular domains with a functionally important flexible helix in the center, or two independent domains that are tethered together by a central linker sequence. A variety of studies have supported the model of two coupled globular domains and the functional importance of key residues in the flexible central helix, including changes in susceptibility to proteolysis (*25*−*27*), functional effects of site-directed mutagenesis (*8*, *9*, *12*−*14*, *19*), kinetics of calcium dissociation (*28*), and site specific probes (*23*, *29*). Recently, scanning calorimetric studies (*30*) showed that the surface electrostatic potential of CaM (*8*) may be a contributor to both CaM's asymmetric functional characteristics, in terms of the order of calcium binding (*19*), and in the coupling between the two globular domains (*30*). Therefore, a variety of experimental data and computational analyses are consistent with a model in which the four calcium binding sites in CaM are functionally coupled in an ordered mechanism of calcium binding, the flexible central helix is functionally important, and there are discrete interactions among the domains. In other words, an increasing body of evidence indicates that CaM is more than the sum of its separate domains.

The enhancement of CaM's affinity for calcium by the RS20 peptide sequence (*19*) is consistent with either model of calcium binding. A more detailed analysis of the change in CaM's calcium binding activity in the presence of the RS20 peptide might allow a further discrimination between the two prevailing models of the calcium binding mechanism, and provide insight into how CaM's enzyme recognition activity and calcium binding activity are functionally linked. In this regard, an examination of how point mutations at the CaM−peptide interface affect the calcium dependence of enzyme activation or CaM's calcium binding activity might provide the required experimental foundations for modeling how these two fundamental features of CaM are linked.

We report here on investigations in which the well-characterized CaM−sm/nmMLCK and CaM−RS20 peptide system was used to gain insight into how CaM's enzyme recognition and calcium binding activities are linked functionally. We found that the basis of RS20 peptide enhance-

ment of CaM's calcium binding activity is through selective effects on each of the four macroscopic Ca^{2+} binding constants of CaM, with the greatest effect being enhanced binding by the two low-affinity sites of CaM. Further, we report here that E84 is a key residue at the CaM−RS20 peptide interface for coupling the peptide recognition and calcium binding activities of CaM, despite being more than 20 Å away from the nearest calcium ligation site in CaM. The results described here were used as the experimental foundation for a more detailed and generalizable computational description of the functional linkage between CaM's calcium and peptide recognition properties.

MATERIALS AND METHODS

Materials

Ultrapure water (Milli-Q system, Millipore) was used in all experiments. Buffers were stored in polyethylene containers pretreated with acid and rinsed with deionized water. Reagents were ACS grade or better. Highly pure $MgCl_2$ and KCl were from Aldrich Chemical Co.; a standard solution of $CaCl_2$ was obtained from Radiometer. $^{45}CaCl_2$ (specific activity of 10.6 mCi/mg) was purchased from ICN.

The CaMs (GenBank accession numbers M11334, AF083237, AF083238, and AF084435) used in this study were produced in *Escherichia coli*, purified, decalcified, and prepared for calcium binding studies using previously described protocols (*19*). The sm/nmMLCK was purified from chicken gizzard tissue (*13*) or produced by recombinant DNA technology (rMLCK1) as previously described (*13*), except for the use of a baculovirus Sf9 polyhedron-virus expression system in place of an *E. coli* system. Briefly, the infected cells were incubated at 27 °C for 72 h prior to harvest and then washed two times with PBS at 22 °C. The washed cells were harvested by gentle scraping and centrifugation at 1000*g* for 20 min at 4 °C. Cell pellets were disrupted by douncing in 2 volumes of buffer A [50 mM Tris-HCl, 5 mM EGTA, 1 mM EDTA, 5 mM DTT, and 5 mM benzamidine (pH 7.5)] on ice. The extract was then centrifuged at 20000*g* for 20 min at 4 °C. The supernatant was applied to a DEAE-cellulose (Whatman DE-52) column previously equilibrated in buffer A without benzamidine. The column was washed with 10 column volumes of buffer A and then step eluted with buffer A containing 150 mM NaCl. Fractions containing the enzyme were pooled; Ca^{2+} was added to a final concentration of 10 mM, and the enzyme was further purified by CaM−Sepharose chromatography (*31*). Fractions containing MLCK activity were made 5 mM in benzamidine and concentrated on a Centriprep 30 (Amicon) concentrator to the desired concentration.

The RS20 peptide analogue (RRKWQKTGHAVRAIGRLSSS-amide) of the CaM binding site of sm/nmMLCK and the CK20 peptide analogue (RRKLKGAILTTMLATRNFSS-amide) of the CaM binding site of CaM-dependent protein kinase II (CaMPKII) were synthesized, purified, and characterized as previously described (*17*).

Methods

Protein and Peptide Concentration Determinations. The concentration of proteins and peptides was determined by amino acid analysis after acid hydrolysis (*19*).

MLCK Activator Assays. The ability of CaMs to activate sm/nmMLCK was determined as described previously (*13*), except that the standard assay conditions at 25 °C were 50 mM HEPES (pH 7.5), 5 mM $MgCl_2$, 150 mM KCl, 15 mM NaCl, 0.2 mM [γ-^{32}P]ATP (specific activity of 200−300 cpm/pmol), 50 μM synthetic peptide substrate (KKRPQRATSNVFAM-amide), 1 mM DTT, and 1 mg/mL bovine serum albumin. The CaM dependence of sm/nmMLCK activation was studied using 1−5 nM sm/nmMLCK and increasing amounts of CaMs in the presence of 0.1 mM $CaCl_2$. Values for the apparent CaM activation constant (K_{CaM}) were calculated from the sm/nmMLCK activation data, using the relationship

$$1/A = 1/A_{max} + K_{CaM}/A_{max}[CaM]$$

where A is sm/nmMLCK activity at a given CaM concentration [CaM] and A_{max} is the maximal sm/nmMLCK activity in the presence of a molar excess of CaM. The [CaM] used in the calculations approximates the [CaM] added under the conditions used here. The average K_{CaM} values were calculated using the linear regression algorithm of InPlot version 4.0 (GraphPad Software Inc.).

Values for the apparent Ca^{2+} binding constant ($K'_{Ca^{2+}}$) were calculated from sm/nmMLCK activation data at various Ca^{2+} concentrations. Experiments were performed using 1−5 nM sm/nmMLCK and 500 nM CaM. Ca^{2+} concentrations in the EGTA-buffered solutions were calculated with a computer program (*32*) based on the reported (*33*) dissociation constants of EGTA and ATP for Ca^{2+} and Mg^{2+}. $K'_{Ca^{2+}}$ values were determined by curve fitting of the Ca^{2+} dependence of sm/nmMLCK activation data, using the relationship

$$A = A_0 + (A_{max} - A_0)/[1 + 10^{(\log K'_{Ca2+} - \log[Ca^{2+}])\alpha}]$$

where A is the sm/nmMLCK activity at a given [Ca^{2+}], A_0 is the sm/nmMLCK activity in the absence of added Ca^{2+}, and α is the Hill slope for the activation curve. For all CaMs studied, A_0 was found to be equal to zero. The average $K'_{Ca^{2+}}$ values were calculated using the nonlinear regression algorithm of InPlot version 4.0 (GraphPad Software Inc.).

Calcium Binding Assays. Calcium binding experiments were performed on decalcified CaM samples by the flow dialysis method (*34*) as described by Haiech et al. (*19*) except the buffer used consisted of 50 mM HEPES, 5 mM $MgCl_2$, 150 mM KCl, and 15 mM NaCl (pH 7.5). In the flow dialysis experiments, the CaM concentration varied from 10 to 60 μM depending upon the mutant studied and the presence of the CaM binding peptides. In experiments with CaM−peptide complexes, the molar ratio of synthetic peptide concentration to that of CaM was 1.5:1. In each experiment, 2−3 μCi of $^{45}CaCl_2$ was used, followed by subsequent additions of unlabeled Ca^{2+} to the flow dialysis chamber each 1.5 min. The dialysis flow rate was 3 mL/min, and fractions were collected in 20 mL scintillation vials at 20 s intervals. Radioactivity was determined by adding 10 mL of Ecoscint A (National Diagnostics) to each vial and counting in a Beckman 6500 liquid scintillation counter. No quenching corrections were applied.

Calculations of Calcium Binding Parameters. To calculate the amounts of bound and free Ca^{2+}, the specific activity of

Ca^{2+} in the flow cell was corrected for the dilution occurring upon the addition of unlabeled Ca^{2+} at each step and the loss of radioactive ligand in the effluent at each step during the course of the experiment. Calcium binding data were fit to sigmoidal titration curves; half-maximal Ca^{2+} binding values, stoichiometry, Hill coefficients, and 95% confidence intervals for these values were calculated using InPlot version 4.0 (GraphPad Software Inc.).

Macroscopic Ca^{2+} dissociation constants for the CaM and CaM−peptide complexes were obtained by fitting the titration data to the Adair−Klotz multisite binding equation (*35*) modified for flow dialysis-derived Ca^{2+} binding data (*36*):

$$y = (ax + 2bx^2 + 3cx^3 + 4dx^4)/(1 + ax + bx^2 + cx^3 + dx^4) + jx \quad (1)$$

where y is the bound Ca^{2+} ratio (moles per mole) and x is the concentration of free Ca^{2+} (micromolar). Terms $a-d$ are defined, for CaMs in the absence of peptide, as follows: $a = 1/K_1$; $b = 1/K_1K_2$; $c = 1/K_1K_2K_3$; $d = 1/K_1K_2K_3K_4$. The terms for CaM−RS20 peptide complexes are as follows: $a = 1/K_1'$; $b = 1/K_1'K_2'$; $c = 1/K_1'K_2'K_3'$; $d = 1/K_1'K_2'K_3'K_4'$. The terms K_1, K_2, K_3, K_4, K_1', K_2', K_3', and K_4' are macroscopic calcium dissociation constants, and j is the slope term for nonspecific binding.

Calcium binding parameters were calculated from at least two experiments for each CaM or CaM−peptide complex.

Fluorescence Assays. Fluorescence titrations of RS20 peptide with wild-type CaM and E84K-CaM were performed using 300 nM RS20 in 50 mM HEPES, 5 mM $MgCl_2$, 150 mM KCl, 15 mM NaCl, and 1 mM $CaCl_2$ (pH 7.5) and a SLM AB2 spectrofluorometer (SLM Instruments, Inc.) with excitation at 295 nm and emission scanned from 310 to 370 nm. Fluorescence intensities were measured following each addition of an aliquot of a CaM stock solution. The emission spectra of E84K-CaM−RS20 and wild-type CaM−RS20 peptide complexes have maxima at 328 and 327 nm, respectively. The fluorescence enhancements are 2.67 for E84K-CaM−RS20 and 2.96 for wild-type CaM−RS20 peptide complexes. Curve fitting was carried out using eq 2, where the fractional fluorescence ($F - F_o/F_{max} - F_o$) was the ordinate and the added CaM/peptide ratio was the abscissa with the nonlinear curve fitting routine of Prism 2.01 (GraphPad Software Inc.). Simulated curves using a Monte Carlo routine for random error for K_D values of 3.5 and 6.8 nM as well as standard simulations of K_D values of 35 and 350 nM and a peptide concentration of 300 nM were obtained using eq 2 and Prism 3.0 (GraphPad Software Inc.).

E84K-CaM−RS20 Peptide Crystallography. The E84K-CaM solution was 24 mg/mL in 25 mM Tris-HCl (pH 7.5); the RS20 peptide solution was 15 mg/mL in water. E84K-CaM−RS20 crystals grew at 4 °C in hanging drops containing 4 μL of CaM solution, 2 μL of RS20 solution, 2 μL of buffer A [20% polyethylene glycol (PEG8000), 100 mM sodium acetate, 5 mM $CaCl_2$, and 0.01% sodium azide, titrated with acetic acid to pH 4.6], and 2 μL of buffer B (same as buffer A but at pH 6.0). One milliliter of buffer A was used for the reservoir solution. Crystals appeared in approximately 10 days. The crystals belonged to space group $P2_1$ with the following dimensions: $a = 61.2$ Å, $b = 40.56$ Å, $c = 32.77$ Å, and $\beta = 91.71°$, with one E84K-CaM−RS20 peptide complex per asymmetric unit. X-ray diffraction data were collected on the Xuong-Hamlin multiwire detection system (*37*). The data were processed with the San Diego Multiwire Systems software (*38*) with a final R_{merge} of 6.49% for all data collected to 1.9 Å resolution.

The E84K-CaM−RS20 structure was determined using molecular replacement methods with the Ca^{2+}-saturated wild-type CaM−RS20 peptide analogue complex (molecule B of PDB file 1CDL) as the search model. This model was judged to have the fewest undefined atoms and the lowest average rms deviation of the four complexes in the asymmetric unit. After multiple cycles of simulated annealing using the program X-PLOR (*39*) and model building using the program O (*40*), the final *R*-factor for the model is 17.1%. This model was refined against 30−1.9 Å data, applying the X-PLOR bulk solvent correction (*41*). The free *R*-factor (*42*) for the final E84K-CaM−RS20 model is 24.2%. The error in the coordinates as estimated using the methods of Luzzati (*43*) and Read (*44*) was 0.2 Å. The final model has one E84K-CaM−RS20 complex per asymmetric unit which contains the 148 residues of E84K-CaM, 4 calcium ions, 20 residues of RS20, 148 ordered water molecules, and 1 ordered acetate molecule from the crystallization buffer. The calculated (*45*) average rms deviations from ideal bond lengths and bond angles are 0.008 Å and 1.117°, respectively. The quality of the electron density map can be seen in the region around the E84K mutation that is shown in Figure 5.

RESULTS

The potential coupling between CaM's Ca^{2+} binding activity and enzyme recognition properties has not been well explored, although it is established that a CaM recognition site peptide from an enzyme, such as the RS20 peptide, allows dissociation of enzyme recognition and enzyme activation with retention of stimulatory effects on calcium binding activity. Among the available point mutations of CaM that are at the interface of CaM's interaction with RS20 peptide, three have been especially useful in both activity and functional analyses. E84K-CaM (accession number AF083237) and E120K-CaM (accession number AF083238) have diminished sm/nmMLCK activator activity (*8*, *9*, *13*), and the combination of the E84K and E120K mutations (e.g., E84K/E120K-CaM; accession number AF084444) abolishes activity (*46*). As a control for discrimination among CaM-regulated protein kinases, the E120K mutation has an effect on the activation of calmodulin-dependent protein kinase II (CaMPKII), whereas the E84K mutation does not. However, the effects of these CaM mutations on the calcium dependence of sm/nmMLCK activator activity have not been reported. Because these types of mutants are unique with their proven ability to identify key residues in CaM's in vitro and in vivo functions (*8*−*14*, *47*), they were used as the starting point in explorations of how perturbation at the CaM−enzyme interface might alter calcium responsiveness and recognition. A detailed analysis of the calcium binding data was carried out to gain insight into how the peptide binding is coupled to calcium binding, and partially uncoupled by the E84K mutation. The resultant computational modeling of the calcium binding data for the wild-type CaM−RS20 and E84K-CaM−RS20 peptide complexes provided a basis for presenting a more detailed mathematical

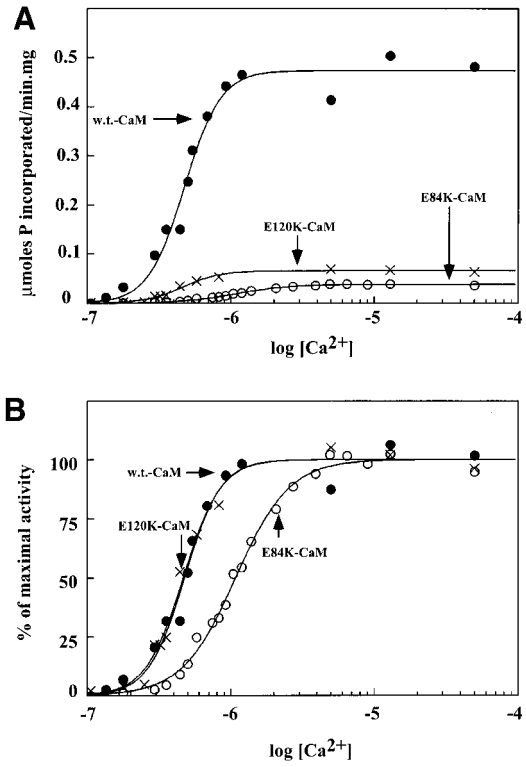

FIGURE 1: Calcium dependence of sm/nmMLCK activation by wild-type and mutant CaMs. MLCK activation curves for wild-type CaM (●), E84K-CaM (○), and E120K-CaM (×) are shown. Plotted on the *X*-axes are calculated free Ca^{2+} concentrations in the EGTA-buffering system (A and B). Plotted on the *Y*-axis are specific activities of sm/nmMLCK (A) or the percent of maximal sm/nmMLCK activator activity for each CaM (B). These experiments were carried out with 33.3 nM CaM and 50 nM sm/nmMLCK (molar ratio of 1:1.5). Each point represents the mean of triplicate measurements. The curves are the best fits of the data to a sigmoidal function as described in Materials and Methods.

description of the linked equilibria that describe the interactions among Ca^{2+}, CaM, and the enzyme, and the determination of the high-resolution crystal structure of the mutant complex provided insight into the structural basis of this functional coupling.

How Do the Functionally Diagnostic Mutants E120K-CaM and E84K-CaM Alter the Calcium Dependence of sm/nmMLCK Enzyme Activation? To determine if either E84K-CaM or E120K-CaM were useful as perturbants of the linkage between CaM's calcium binding and enzyme recognition properties, the calcium dependencies of activation by the two mutant CaMs and wild-type CaM were compared. While both E84K-CaM and E120K-CaM are contact residues and have reduced sm/nmMLCK activator activities compared to wild-type CaM, only E84K-CaM requires a higher concentration of calcium to attain its maximal activity (Figure 1).

It could not have been predicted in advance that E84 would be more important than E120 in CaM's calcium dependence of sm/nmMLCK regulation. Neither residue is close to the calcium binding sites of CaM, and both have been found to be peptide contact residues in the crystal structure of the CaM−RS20 peptide analogue complex. The apparent Ca^{2+} binding constant ($K'_{Ca^{2+}}$) for sm/nmMLCK activation (see Materials and Methods) by E84K-CaM is 0.69 ± 0.02 μM, compared to 0.17 ± 0.02 μM for wild-type CaM. The apparent CaM activation constant, K_{CaM} (see Materials and Methods), is 5.0 ± 0.4 nM for E84K-CaM, compared to 1.4 ± 0.7 nM for wild-type CaM. In other words, a 4-fold change in $K'_{Ca^{2+}}$ is correlated with a 3.6-fold change in K_{CaM}.

The experimentally determined relationship between $K'_{Ca^{2+}}$ and K_{CaM} is unexpected on the basis of the generally accepted descriptions of the calcium dependence of enzyme activation by CaM. The scheme that has traditionally been used to describe the relationships among Ca^{2+} binding and enzyme (E) interaction with CaM and to calculate the commonly used $K'_{Ca^{2+}}$ and K_{CaM} values is as follows (*50*) (Scheme 1):

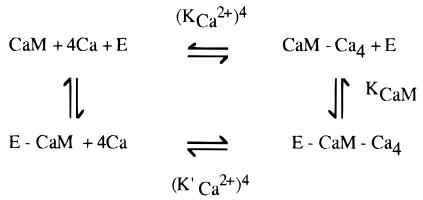

where K_{CaM} is the apparent CaM activation constant for the enzyme (E), $K_{Ca^{2+}}$ is the apparent Ca^{2+} binding constant for the interaction of Ca^{2+} with CaM, and $K'_{Ca^{2+}}$ is the apparent Ca^{2+} binding constant for the interaction of Ca^{2+} with the CaM−enzyme complex. If the E−CaM−Ca_4 is the only active species, then any changes in $K'_{Ca^{2+}}$ must be raised to the fourth power to be proportional to changes in K_{CaM}. Therefore, the observed 4-fold change in $K'_{Ca^{2+}}$ seen with the CaM point mutation (E84K) at the CaM−peptide interface should have resulted in the K_{CaM} for sm/nmMLCK−E84K-CaM being changed by 256-fold [$=(0.69/0.17)^4$], rather than the observed 3.6-fold.

The results require that key assumptions be examined to determine why the experimental results do not correlate with the expected results. For example, the existing models (see ref *1*) allow only for an all-or-none effect of enzyme binding; i.e., there is not a provision for variable coupling between peptide and Ca^{2+} binding. Thus, any effect of an interface mutation on Ca^{2+} binding would be simply due to the failure to form a CaM−enzyme complex. In addition, it is assumed that the Ca^{2+} binding properties of wild-type CaM and E84K-CaM would be similar because the mutation is not in a calcium binding site of CaM. As the next step in our investigation, we tested the validity of some of these assumptions.

Is the Change in Calcium-Dependent Enzyme Activation Due to a Change in the Calcium Binding Activity of E84K-CaM? One of the more straightforward assumptions that can be checked by direct ligand binding using flow dialysis is that a mutation of CaM outside of a calcium ligation structure can alter the calcium binding activity. A comparison of the Ca^{2+} binding properties of wild-type CaM and E84K-CaM was carried out under the same conditions that were used for enzyme activation analysis. As shown in Figure 2, the calcium binding curves of wild-type CaM and E84K-CaM are essentially superimposable, and plateau at a stoichiometry of 4. Therefore, the results are consistent with the calcium binding activity of wild-type and mutant CaMs being similar, and do not provide an explanation for the deviation of the experimental results in Figure 1 from the expected values for K_{CaM}. However, these results do not address the possibility that the calcium binding properties of E84K-CaM might differ from those of wild-type CaM if examined as part of a complex with a CaM binding structure.

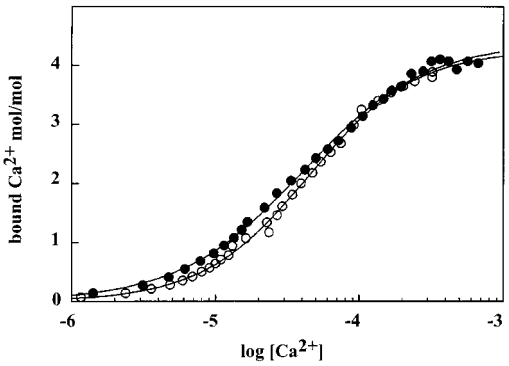

FIGURE 2: Ca^{2+} binding properties of wild-type and mutant CaMs. Representative Ca^{2+} binding curves of wild-type CaM (●) and E84K-CaM (○) are shown. The curves are the best fit of the data to a sigmoidal function as described in Materials and Methods.

Is the Change in Calcium-Dependent Enzyme Activation Due to a Change in the Calcium Binding Activity of E84K-CaM When It Is Part of a Complex? Related to This, Does a Mutation at the Interface Partially Uncouple the Enhancement of CaM's Calcium Binding Activity by a CaM Recognition Site Peptide? The sm/nmMLCK or its CaM recognition site peptide, RS20 peptide, can enhance the calcium binding activity of CaMs. This raises the logical possibility that the Ca^{2+} binding activity of the E84K-CaM might differ from that of wild-type CaM when associated with a CaM binding structure. Although E84 is more than 20 Å away from the nearest calcium binding site, it is theoretically possible that E84 might alter Ca^{2+} binding activity of the CaM−RS20 peptide complex through a critical functional role at the CaM−peptide interface. To directly address this possibility, the calcium binding activities of the E84K-CaM−RS20 peptide complex and that of the wild-type CaM−RS20 peptide complex were compared to each other and to those of CaMs in the absence of RS20 peptide.

As shown in Figure 3A, the E84K-CaM−RS20 peptide complex exhibited an 8.5-fold increase in overall calcium binding affinity, whereas the wild-type CaM−RS20 peptide complex showed about a 30-fold increase in Ca^{2+} binding affinity compared to either CaM alone. However, the change in the Hill coefficient for the calcium binding curves for CaMs compared to those for the CaM−RS20 peptide complexes is similar. That is, the values for both wild-type CaM and E84K-CaMs are changed from 1.2 to 1.7 in the presence of RS20 peptide. This is suggestive of an effect of the E84K mutation that is not all-or-none with respect to Ca^{2+} binding enhancement. This point is addressed in a following section.

The reduced enhancement of the Ca^{2+} activity of E84K-CaM−RS20 peptide complex compared to that of wild-type CaM−RS20 peptide complex is a selective effect in that the Ca^{2+} binding properties of the E120K-CaM−RS20 peptide complex (Figure 3A) are essentially identical to that of the wild-type CaM−RS20 peptide complex, even though E120K is also a peptide contact residue. In addition, when E82K-CaM (accession number AF084435) was tested for Ca^{2+} dependence of sm/nmMLCK activation and Ca^{2+} binding activity, it was found to be indistinguishable from wild-type CaM (data not shown). E82 is not a peptide contact residue in CaM, but is located proximal to E84 in the same helix structure. Therefore, the decreased calcium binding activity

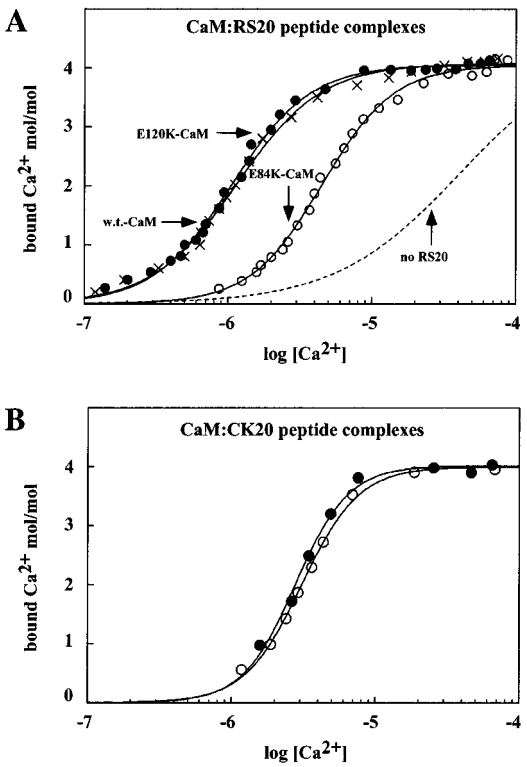

FIGURE 3: Ca^{2+} binding properties of wild-type and mutant CaMs in the presence of CaM recognition peptides. (A) Ca^{2+} binding curves from representative experiments with complexes containing RS20 and either wild-type CaM (●), E84K-CaM (○), or E120K-CaM (×) are shown. Curves were generated by the best fit of the data to a sigmoidal function as described in Materials and Methods. The dashed line indicates the relative position of the calcium binding curve for wild-type CaM or E84K-CaM in the absence of RS20 (see Figure 2). (B) Ca^{2+} binding curves from representative experiments with complexes containing CK20 peptide and either wild-type CaM (●) or E84K-CaM (○) are shown. Flow dialysis experiments were performed, and curves were generated by best fit of the data to a sigmoidal function as described in Materials and Methods.

of the E84K-CaM−RS20 peptide complex is a selective effect that cannot be mimicked by similar mutations of glutamic acids that are in the same helix as E84, or by similar mutations of another glutamic acid that is a peptide contact residue.

Although the data clearly demonstrate a key role for E84 in linking CaM's calcium binding activity to its calcium-dependent regulation of sm/nmMLCK, it is reasonable to ask if this key role for E84 is potentially a general feature, or selective for those enzymes which report a functional effect of the E84K mutation. As an initial test of this question about enzyme selectivity, the calcium binding activity of E84K-CaM complexed with the CaM recognition sequence from CaMPKII (CK20 peptide) was examined because of this enzyme's known resistance (*8*, *13*) to the E84K mutation in CaM. As shown in Figure 3B, the calcium binding activities of mutant and wild-type CaMs complexed with CK20 peptide are similar. In addition, the difference in the affinity of Ca^{2+} binding by the CaM−CK20 peptide complex compared to that of the CaM−RS20 peptide complex is consistent with the differences in Ca^{2+} sensitivity of the parent kinases. Therefore, the effect on the calcium binding activity of E84K-CaM in a complex is a feature that shows selectivity among CaM recognition site peptides, possibly

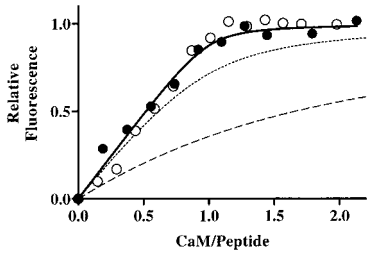

FIGURE 4: RS20 peptide binding properties of wild-type CaM and E84K-CaMs. Analysis of RS20 peptide binding by monitoring the fluorescence change in the single tryptophan residue of RS20 was carried out as described in Materials and Methods. Binding data were generated by titration of RS20 (300 nM) with increasing amounts of wild-type CaM (●) or E84K-CaM (○). The curve fitting routine (see Materials and Methods) yielded direct estimations of K_D values with an R^2 of >0.98 for both wild-type CaM (3.5 ± 1.9 nM) and E84K-CaM (6.8 ± 5.2 nM). Data shown are from one representative experiment for each CaM. Plotted on the *X*-axis are the molar ratios of CaM to RS20 peptide; plotted on the *Y*-axis are the fractions of maximal enhancement of fluorescence intensity upon RS20 binding for each CaM. To ascertain the sensitivity of the assay method to changes in K_D, simulated curves (see Materials and Methods) for K_D values 10- and 100-fold higher than that of wild-type CaM were generated. The dotted line shows the simulated curve for a K_D of 35 nM, and the dashed line shows the simulated curve for a K_D of 350 nM.

reflecting whether the CaM mutation affects the particular enzyme activity.

Can the Loss of Calcium Binding Activity Seen with a Point Mutation at the CaM−Peptide Interface Be Explained Simply by the Loss of Peptide Binding Activity? An obvious explanation, based on more simplified models of the interactions between CaM and recognition site peptides, is that the decreased ability of RS20 peptide to enhance E84K-CaM's Ca^{2+} binding activity compared to that of wild-type CaM is due to a corresponding loss of RS20 peptide binding activity by E84K-CaM. There is a 4-fold difference in the Ca^{2+} dependence of sm/nmMLCK activation and a similar difference in the Ca^{2+} affinity of the two CaM−peptide complexes. As discussed above, the predicted change in peptide binding affinity is therefore expected to be at least 4^4- or 256-fold if the linkage between calcium binding and enzyme recognition is simply the ability to form a CaM−Ca_4 complex (all-or-none model). However, this prediction does not consider coupling among the various calcium binding events and between each calcium binding event and peptide binding. To test the validity of prevailing models and potentially gain insight into the mechanism, we directly compared the binding of RS20 peptide to wild-type CaM and E84K-CaM to see if there was a greater than 200-fold loss of RS20 peptide binding activity.

The binding of RS20 peptide to CaM can be conveniently monitored due to the fluorescence properties of the single tryptophan residue in the peptide. The tryptophan emission spectrum of RS20 peptide undergoes a blue shift (355 to 327 nm) for both wild-type CaM and E84K-CaM complexes characteristic of a tryptophan residue placed in a hydrophobic environment. In addition, the fluorescence signal is enhanced to comparable levels in both the wild-type and E84K-CaM complexes. Results of fluorescence monitoring of additions of wild-type CaM and E84K-CaM to RS20 peptide in the presence of saturating Ca^{2+} are shown in Figure 4.

The data for RS20 peptide binding by both wild-type CaM and E84K-CaM plateau at CaM/RS20 peptide ratios close to 1.0, and clearly do not reveal a 256-fold difference. To obtain the dissociation constants, fluorescence data from 336 to 338 nm were averaged and fit to the nonlinear equation (*48*)

$$F - F_o/F_{max} - F_o = 0.5\{x/E + K/E + 1 - [(x/E + K/E + 1)^2 - 4x/E]^{1/2}\} \quad (2)$$

where F is the fluorescence intensity for each titration point, F_{max} is the maximal fluorescence intensity of the CaM−RS20 peptide complex, F_o is the fluorescence intensity of the peptide in the absence of CaM, K is K_D (the dissociation constant for the CaM−RS20 peptide complex), x is the concentration of CaM added, and E is the initial concentration of RS20 peptide (300 nM). Dissociation constants from two independent experiments for each CaM were averaged. The calculated K_D values for wild-type CaM and E84K-CaM are 3.5 ± 1.9 and 6.8 ± 5.2 nM, respectively. The K_D value for wild-type CaM is comparable to values calculated previously from competition/inhibition binding experiments (*17*, *49*).

To address the question of assay discrimination (i.e., can a 256-fold difference be detected), we generated simulation curves with random error in the data for each of the average K_D values (see Materials and Methods). Simulated curves at K_D values 10- or 100-fold higher than that of wild-type CaM were shifted to the right and readily distinguishable from the experimental data (Figure 4). Thus, the method would be able to distinguish differences much smaller than 256-fold, indicating that the differences in Ca^{2+} binding between wild-type CaM−RS20 and E84K-CaM−RS20 peptide complexes cannot be explained solely by a difference in the RS20 peptide binding to Ca^{2+}-saturated CaMs. Therefore, an explanation of the results in Figures 3 and 4 requires an expanded description that considers a variable effect of peptide interactions on calcium binding. As described in a subsequent section, an expansion of the Adair−Klotz equation allows a mathematical description of the relationship between calcium binding and peptide binding activity.

Could the Enhancement of CaM's Ca^{2+} Binding Activity by RS20 Peptide and Its Partial Uncoupling in E84K-CaM Be a Reflection of Discrete Effects on CaM's Ca^{2+} Binding Activity? The results with the E84K-CaM−RS20 peptide complex indicate a partial uncoupling of RS20 peptide's ability to enhance CaM's calcium binding activity. However, current models of Ca^{2+} binding by CaM do not provide an explanation for how RS20 peptide binding might enhance CaM's Ca^{2+} binding activity, much less its partial uncoupling by a mutation at the CaM−peptide interface that is so remote from a calcium binding site. As a first step toward gaining insight into parameters that might be important in such a model, we subjected the experimental data to a more detailed analysis which considers the interactions between partially saturated CaM and enzyme and/or peptide presented in Scheme 2:

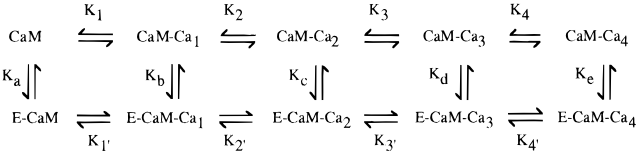

Table 1: Macroscopic Ca^{2+} Dissociation Constants[a] for CaMs and CaM−RS20 Peptide Complexes.

CaM	RS20 peptide	$K_1(K_1')$ (μM)	$K_2(K_2')$ (μM)	$K_3(K_3')$ (μM)	$K_4(K_4')$ (μM)	ΔG^b (kcal/mol)
wild-type	no	15.0 ± 2.0	13.0 ± 0.9	82.4 ± 8.4	102.0 ± 9.2	−24.3
wild-type	yes	0.4 ± 0.1	2.5 ± 0.2	0.8 ± 0.2	1.1 ± 0.1	−32.8
E84K	no	16.6 ± 4.0	23.4 ± 4.3	111.3 ± 4.1	45.4 ± 4.5	−24.2
E84K	yes	5.1 ± 1.9	3.2 ± 1.0	4.6 ± 1.3	5.8 ± 0.6	−29.2

[a] Ca^{2+} binding by CaMs and CaM−RS20 peptide complexes was studied using flow dialysis (see Figures 2 and 3A) under the standard experimental conditions [50 mM HEPES, 150 mM KCl, 15 mM NaCl, and 5 mM $MgCl_2$ (pH 7.5)] as described in Materials and Methods. Macroscopic dissociation constants (K_n for CaMs or K_n' for CaM−RS20 peptide complexes) were determined by fitting the data to the Adair−Klotz equation for four-site cooperative binding (eq 1). $R^2 = 0.999$ for wild-type CaM and E84K-CaM; $R^2 = 0.998$ for wild-type CaM−RS20 and E84K-CaM−RS20 peptide complexes. [b] The free energy of calcium binding ΔG was calculated with the equation $\Delta G = RT \ln K_1K_2K_3K_4$, where R is the gas constant and T is 298 K.

where K_1-K_4 are dissociation constants for Ca^{2+} binding by CaM and $K_1'-K_4'$ are the corresponding dissociation constants for Ca^{2+} binding by each CaM−E complex. K_a-K_e are the association constants for the interaction of E (enzyme or CaM binding peptide) with CaM.

Ca^{2+} binding data for uncomplexed wild-type CaM and E84K-CaM and their complexes with RS20 peptide were analyzed using the Adair−Klotz equation for multisite ligand interactions (eq 1; see Methods). This allowed an estimation of how the individual macroscopic Ca^{2+} dissociation constants might be altered by a CaM binding structure.

The estimated macroscopic calcium dissociation constants for CaM and CaM−RS20 peptide complexes are listed in Table 1. This more detailed analysis indicates an enhancement of approximately 100-fold for two lower-affinity macroscopic dissociation constants of wild-type CaM (comparison of K_3 and K_4 to K_3' and K_4'). Two other macroscopic dissociation constants (comparison of K_1 and K_2 to K_1' and K_2') are also enhanced between 5- and 37-fold in the wild-type CaM−RS20 peptide complex. The calculated macroscopic constants allow one to estimate an overall ΔG for the calcium binding by CaM or by the CaM−RS20 peptide complex (Table 1). The difference in computed ΔG values for the wild-type CaM−RS20 peptide and wild-type CaM alone (−8.5 kcal/mol) represents the free energy of coupling (*50*) and is indicative of the overall difference in energetics of Ca^{2+} binding by CaM compared to that by the CaM−RS20 peptide complex.

The computed values in Table 1 reveal no net effect of the E84K mutation on calcium binding by uncomplexed CaM, consistent with the lack of a difference in the overall calcium binding activity between wild-type CaM and E84K-CaM (Figure 2). Similarly, smaller effects of RS20 peptide on the individual constants for E84K-CaM (Table 1) are consistent with the RS20 peptide only increasing the affinity of E84K-CaM by 8.5-fold compared to the 30-fold change observed for wild-type CaM (Figure 3A). Specifically, the RS20 peptide only increases the macroscopic calcium dissociation constants of E84K-CaM (comparison of K_1, K_2, and K_4 to K_1', K_2', and K_4', respectively) between 3- and 8-fold. The greater enhancement (24-fold) is calculated only for one lower-affinity macroscopic dissociation constant (comparison of K_3 to K_3'). The computed free energy of coupling for the E84K-CaM−RS20 peptide complex is −5.0 kcal/mol. Overall, the difference in the energetics of coupling between the two complexes (wild-type CaM−RS20 peptide vs E84K-CaM−RS20 peptide) is approximately −3.5 kcal/mol. This magnitude of the free energy difference would be consistent with a change of perhaps one or two hydrogen bonds or ion pairs, suggestive of discrete structural changes (addressed in the last section of the Results).

Table 2: Peptide−Calcium Coupling Factors[a] for CaM−Ca_n−RS20 Peptide Complexes

CaM−RS20 peptide complex	C_1	C_2	C_3	C_4
wild-type CaM−RS20 peptide	40.6	5.2	112.3	82.7
E84K-CaM−RS20 peptide	3.3	7.0	37.0	5.4

[a] Peptide−calcium coupling factors (C_1-C_4) were calculated by fitting Ca^{2+} binding data for CaM−RS20 peptide complexes to the modified Adair−Klotz equation (eq 3) using macroscopic dissociation constants K_1-K_4 from Table 1.

Can an Expanded Version of the Generalizable Adair−Klotz Equation Describe the Calcium Binding Data and the Coupling of Ca^{2+} and Peptide Binding Events? As mentioned above, an expansion of the mathematical description of Ca^{2+} binding is necessary for determining how Ca^{2+} binding and peptide binding are quantitatively coupled. A need for expansion of the Adair−Klotz equation was proposed by Klotz (*51*) to enable a mathematical description for multisite binding of ligands to receptors. This is especially needed in cases where the binding of one ligand affects the binding affinity of another ligand, and where allosteric effects due to protein conformation changes (e.g., arising from either a second protein interaction or dimerization) must be accounted for in the ligand binding process. In the CaM−peptide complexes, both of these conditions are operative. Using other terms, the calcium−CaM−RS20 peptide system has both homotropic (between calcium binding events) and heterotropic (between calcium and peptide binding events) linkages. The expansion of the Adair−Klotz equation to more accurately fit the experimental data for such complexes is presented below and includes the introduction of coupling terms:

$$y = (C_1x/K_1 + 2C_1C_2x^2/K_1K_2 + 3C_1C_2C_3x^3/K_1K_2K_3 + 4C_1C_2C_3C_4x^4/K_1K_2K_3K_4)/(1 + C_1x/K_1 + C_1C_2x^2/K_1K_2 + C_1C_2C_3x^3/K_1K_2K_3 + C_1C_2C_3C_4x^4/K_1K_2K_3K_4) + jx \quad (3)$$

where y is the amount of bound Ca^{2+} (moles per mole) for the CaM−RS20 peptide complex, x is the concentration of free Ca^{2+}, K_1-K_4 are macroscopic calcium dissociation constants for CaM in the absence of peptide, C_n are the coupling factors applied to each stoichiometric macroscopic constant of the uncomplexed CaM, and j is a nonspecific binding term. The calculated coupling factors derived from the experimental data are shown in Table 2.

The expanded equation makes no assumptions about the mechanism of Ca^{2+} binding, only that an external ligand (e.g., peptide or protein) can affect each Ca^{2+} binding parameter. Ca^{2+} binding data obtained for the CaM and CaM−peptide complexes can be fit to this expanded equation, allowing solution for the coupling factors associated with each macroscopic constant. However, the observation that coupling between peptide and calcium binding is found at all

four Ca^{2+} binding events is consistent with the accumulating body of evidence that supports a sequential and cooperative mechanism for this process. The coupling between calcium and peptide binding in the wild-type CaM and RS20 peptide system is largest in C_3 and C_4 terms, which are associated with the lower-affinity sites. These results support the hypothesis that the affinity for the peptide increases as more Ca^{2+} is bound, and concurrently, the Ca^{2+} affinity increases as interactions with the peptide are enhanced. Thus, the introduction of coupling factors allows one to describe by the use of a generalizable equation the observed effects of peptide binding on CaM's macroscopic calcium dissociation constants.

In addition to describing the effect of RS20 peptide on the Ca^{2+} binding behavior of wild-type CaM, the expanded equation can also be used to describe the effects on the E84K-CaM (Table 2). Like with the wild-type CaM, the effect of RS20 peptide is seen at four Ca^{2+} binding events. In contrast to wild-type CaM, the effect of RS20 peptide on the Ca^{2+} binding activity of E84K-CaM is smaller than on wild-type CaM at three of the four coupling factors. Differences in coupling factors between wild-type CaM and E84K-CaM are largest at C_1 (12-fold) and C_4 (15-fold). These demonstrate the partial uncoupling of peptide and Ca^{2+} binding that occurs as a result of the E84K mutation and suggest that the effect is distributed among several sites.

If certain assumptions are made, then changes in coupling factors can be associated with certain Ca^{2+} binding sites. The first assumption is that the same ordered-sequential Ca^{2+} binding mechanism is operative in both wild-type CaM and E84K-CaMs and their respective RS20 peptide complexes. The second assumption is that the macroscopic constants reflect apparent site constants. Previous studies (*23*, *24*, *30*) have shown that macroscopic Ca^{2+} binding constants for CaM can be associated with discrete sites. It is reasonable to extend this relationship to the data for Ca^{2+} binding in the presence of RS20 peptide because the values reported here were obtained under identical conditions and with a molar excess of peptide at least 1000-fold greater than the K_D for CaM and peptide. According to the sequential mechanism, the order of binding is first to structural site III followed by sites IV, I, and II. Thus, coupling factors corresponding to the mechanistic first and fourth calcium binding events (C_1 and C_4) of CaM can be associated with the third and second calcium binding structures from the amino terminus. These are the two sites closest to the middle of the molecule. E84 is located in the helix that precedes calcium binding structure III, the first site to be occupied in the mechanism. Thus, the differences in the coupling factors are entirely consistent with the structural and mechanistic data.

Analysis of the experimental data by using the expanded Adair−Klotz equation shows that the E84K mutation affects the overall binding of Ca^{2+} to the CaM−RS20 peptide complex by altering the linkage of Ca^{2+} binding with peptide interaction at multiple steps in the Ca^{2+} binding process. The coupling factors, C_n, are proportional to ratios of peptide binding constants through the relationships $C_1 = (1 + K_bE)/(1 + K_aE)$, $C_2 = (1 + K_cE)/(1 + K_bE)$, $C_3 = (1 + K_dE)/(1 + K_cE)$, and $C_4 = (1 + K_eE)/(1 + K_dE)$, where K_a, K_b, K_c, K_d, and K_e are the apparent association constants of the five possible complexes of CaM and RS20 with zero to four Ca^{2+} bound and E is the free peptide concentration (see Scheme 2 above).

Inspection of the resultant calculations offers insight into why a large change in peptide binding by Ca^{2+}-saturated CaM is not required for an effect on calcium binding. For example, coupling factor C_4 differs by about 15-fold between the two complexes (Table 2). An increase in K_d, the peptide association constant for E84K-CaM complexes containing three bound calcium ions, can be a major contributor to the decrease in C_4 between wild-type CaM and E84K-CaM complexes. A similar argument can be made for a change in K_a and/or K_b because the respective C_1 values differ by more than 12-fold between wild-type CaM−RS20 and E84K-CaM−RS20 peptide complexes. Previous models for Ca^{2+} binding did not account for both increases and decreases in peptide association constants for the various Ca^{2+}−CaM−peptide complexes. Only by considering the coupling at each step in the Ca^{2+} binding mechanism can these changes in Ca^{2+} and peptide interaction be rationalized.

Does the E84K Mutation in CaM Result in a Major Change in Polypeptide Chain Fold in the CaM−RS20 Peptide Complex? E84 of CaM is partially buried and in close association with a complementary charge environment of the peptide in the previously reported (*18*) wild-type complex. Therefore, the introduction of a charge reversal perturbation in E84K-CaM has the potential to produce a significantly different fold of the CaM−peptide complex. This new fold could, in theory, retain peptide binding activity. Alternatively, it is possible that a comparatively subtle change at the CaM−peptide interface could compensate for the charge reversal mutation in CaM. Precedents in the literature are consistent with the latter model in which α helices have an apparent plasticity that allow for mutations or alternative sequences to be accommodated with retention of overall polypeptide fold (*52*−*55*). Regardless, insight into the structural basis of the functional changes requires that the high-resolution structure of the E84K-CaM−RS20 peptide complex be determined. Therefore, we elucidated the crystal structure of the calcium-saturated E84K-CaM−RS20 peptide complex to distinguish among possibilities and gain more detailed knowledge about this mutant CaM which has provided so many insights into CaM function and activity.

The X-ray crystallographic structure of the E84K-CaM−RS20 peptide complex was refined to 1.9 Å resolution. The structure was determined using molecular replacement methods with a previously reported (*18*) Ca^{2+}-saturated complex as a search model (molecule B of PDB file 1CDL). After multiple cycles of refinement and model building, the *R*-factor for the E84K-CaM−RS20 peptide model was 17.1%, and the free *R*-factor (calculated from data not used in the refinement) for the final model was 24.1%.

Comparison of the wild-type CaM and mutant CaM−RS20 peptide structures indicates that the conformation of the individual domains of CaM and the orientation of the CaM binding peptide are well conserved between E84K-CaM−RS20 peptide and wild-type CaM−RS20 peptide analogue complexes, with an rmsd ranging from 0.8 to 0.9 Å. There is not a global change in the structure resulting from the E84K mutation, consistent with the fluorescence properties and RS20 peptide binding affinity exhibited by E84K-CaM. The differences between the structures are largely localized to the helix containing K84. In the wild-type structure, the

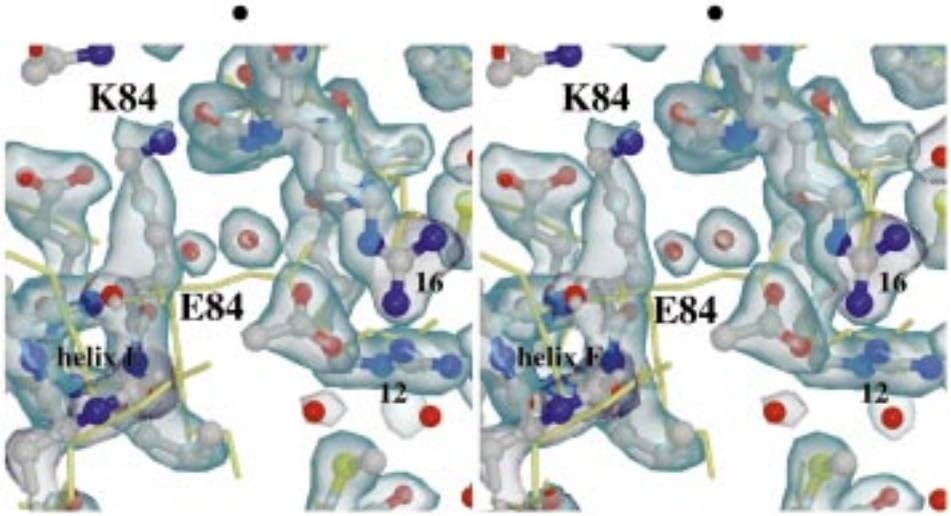

FIGURE 5: E84K-CaM−RS20 peptide complex structure in the vicinity of the mutation. Shown is a stereoview of the molecule oriented such that helix E containing K84 of the E84K-CaM−RS20 peptide complex (ball-and-stick) is directed into the page. A $2F_o - F_c$ electron density map of the complex is shaded around the atoms visible in this view. The same region of the wild-type CaM−RS20 peptide analogue complex (yellow sticks) is shown for comparison. The 1.9 Å resolution E84K-CaM−RS20 peptide complex was superimposed on the 2.4 Å resolution wild-type CaM−RS20 peptide analogue complex (Protein Data Bank file 1CDL chain B, CaM, and chain F, peptide) by alignment of CaM residues 91−145 and peptide residues 4−17. The ordered acetate molecule and several water molecules are also present in the vicinity of the mutation. The presence of acetate does not affect Ca^{2+} binding by wild-type CaM−RS20 or E84K-CaM−RS20 peptide complexes (data not shown). Numbers 12 and 16 correspond to arginines of RS20 peptide making contacts with residue 84 in the wild-type CaM complex.

side chain carboxylate of E84 makes hydrogen bond contacts (3.0 ± 0.2 Å) with a pair of arginine side chains from RS20. However, in the E84K-CaM−RS20 peptide complex, residue 84 is rotated away from the peptide (Figures 5 and 6A). The average distance from the terminal nitrogen of the K84 side chain to the nitrogen atoms of peptide arginines is 9.0 ± 1.0 Å. Thus, the movement of the side chain of K84 eliminates a charge−charge conflict in the structure.

Another difference between the structures is in the angle that helix E of CaM, containing residue 84, makes with respect to the C-terminal domain. This appears to be the result of a rotational movement of this helix away from the peptide (Figures 5 and 6). This movement could potentially influence the binding of Ca^{2+} to CaM, especially at calcium ligation structure III.

DISCUSSION

Insight into possible mechanisms for how a CaM binding structure can enhance the calcium binding activity of CaM has been gained by a detailed analysis of CaM's calcium binding events and their linkage to enzyme or peptide binding and enzyme regulation. While the specific case study used was that of sm/nmMLCK and its CaM recognition site peptide, the approaches can be extended to most CaM-regulated enzymes and a diversity of multiligand binding systems. The demonstration that E84 is a key functional residue in CaM that links its calcium binding activity with enzyme binding and regulation, however, is probably restricted to those CaM-regulated enzymes for which mutation of E84 has resulted in a selective effect on enzyme recognition and activation (*9*−*13*). Regardless of the restriction of the results with E84 changes to a subset of CaM-regulated proteins, the combination of utilizing charge perturbation mutagenesis at a CaM−enzyme interface and detailed ligand binding analysis is one that can be extended to all CaM-regulated enzymes. Similar charge perturbation mutagenesis approaches have been used in other multisubunit enzyme systems (*56*, *57*), demonstrating the potential for combining direct ligand binding with perturbing, but not lethal, mutations at protein−protein interfaces. Knowledge about quantitative linkages between ligand binding sites and receptor interactions with other proteins is required to gain further insight into how the binding of small molecules, such as ions and drugs, might be functionally coupled to the modulation of macromolecular interactions that amplify or transduce the stoichiometric interaction into a biological response.

A unique aspect of this study is the use of the same conditions to analyze the calcium-dependent enzyme activation, calcium binding activity, and peptide recognition. As noted recently (*1*), it is imperative to carry out such comparative measurements under identical conditions to establish the significance of quantitative functional changes and gain insight into molecular mechanisms. The common conditions used here approximate those of the vertebrate intracellular environment. The effects on calcium binding activity and calcium dependence of enzyme activation under the same conditions are not seen with a variety of control mutations, thereby providing a strong correlation between the functional significance of E84 for sm/nmMLCK regulation and its location within the CaM−RS20 peptide complex. The results with calcium-dependent enzyme activation and calcium binding activity are consistent with each other, and provide the foundation for a more detailed model of how calcium binding activity and enzyme recognition and regulation are coupled.

It is proposed that sm/nmMLCK and related enzymes enhance the calcium binding activity of CaM through a differential effect on each of the four calcium binding sites, with the greatest effect being on the low-affinity calcium binding sites of CaM. Further, E84 is one of several interface residues that are functionally more important than others due

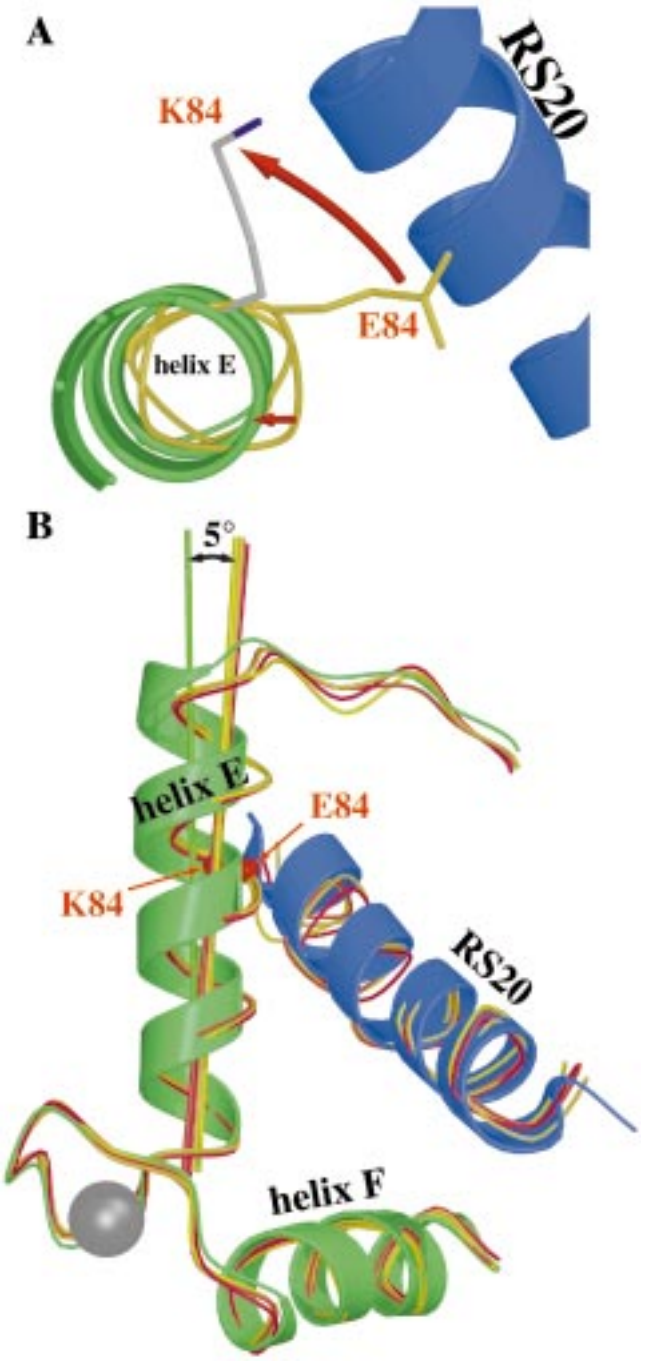

FIGURE 6: Comparison of the relative position of helix E in wild-type CaM and E84K-CaM in complexes with MLCK-based peptides. The orientation of helix E in E84K-CaM is rotated 5° from its relative position in the wild-type CaM when the two structures for CaM−peptide complexes are compared. The plane in which the 5° variation occurs is different from the variation seen among the different molecules within the asymmetric unit of the CaM−RS20 peptide complex, indicating that this small change is not simply a reflection of experimental variance. Only the peptide and the relevant Ca^{2+} binding structure of CaM are displayed. Helices E and F (green ribbon) of E84K-CaM are shown along with the helical RS20 peptide (blue ribbon). The model for E84K-CaM is that presented for the 1.9 Å resolution structure in this report. The model for wild-type CaM is that from the 2.4 Å resolution structure (1CDL) reported previously (*18*). (A) In the same orientation as in Figure 5, a portion of helix E of each CaM is shown as a trace following the Cα of each residue. The difference in the position of the side chain at residue 84 and the shift in the N-terminus of helix E are indicated by the red arrows. (B) The molecules are rotated 90° around the horizontal as compared to the view in panel A. All four complexes in the wild-type crystal structure 1CDL (PDB) are used for comparison. The Cα trace for each molecule in the asymmetric unit of the 1CDL database file is shown as a colored coil (yellow, yellow-orange, orange, and red).

to their role in coupling the calcium binding and enzyme recognition properties of CaM. Computation of the free energy of coupling for individual Ca^{2+} events indicates that the E84K-CaM−RS20 peptide complex has perturbed coupling at sites represented by coupling factors C_1 and C_4, which correspond to the first and last Ca^{2+} binding events, respectively.

Of considerable interest here is the crystallographic structure determination for the E84K-CaM−RS20 peptide complex, which shows that the structure of the mutant complex is not dramatically different compared to the wild-type CaM−RS20 peptide analogue complex. The change in the structure is essentially localized to the site of mutation and alters the orientation of the helix containing the mutated residue. The effect of the E84K mutation on the movement of the helix is particularly interesting because residue 84 precedes calcium binding structure III which is the initial site occupied by calcium in the proposed sequential cooperative mechanism in uncomplexed CaM. The estimated calcium binding energy difference between E84K-CaM−RS20 and wild-type CaM−RS20 peptide complexes available from this study (−3.5 kcal/mol), and the distribution of the E84K mutation's effect across multiple dissociation and coupling events, make specific structural correlations difficult. However, precedents in regulatory biology unrelated to CaM-regulated pathways have shown (*58*−*60*) that alterations in protein function can be related to changes of a fraction of an angstrom in amino acid side chain positions, and that α-helices can make localized changes in structure as an adaptation to perturbing mutations with retention of protein fold. Analysis of the experimental data with the expanded Adair−Klotz equation revealed that the major effect of the E84K mutation is on coupling factor C_1, which is correlated with the first Ca^{2+} binding event that occurs at Ca^{2+} binding structure III. Therefore, alterations in the behavior of Ca^{2+} binding structure III are anticipated on the basis of the structure, and alterations in the ion binding properties of this first mechanistic site are expected, in turn, to make a contribution to the affinity of each of the subsequent sites on the basis of the relationships described by the expanded Adair−Klotz equation.

In conclusion, the precedent reported here raises the possibility that there may be a redundant theme used in CaM-regulated signal transduction pathways in which certain residues at the CaM−enzyme interface are more critical than others in modulating the link between calcium binding activity and enzyme regulation. Our results add to a growing body of knowledge that indicates that each CaM−enzyme complex can differentially contribute to the net response of a eukaryotic cell to an intracellular calcium signal as a result of their differential calcium responsiveness, adaptability, and localization. For example, sequences outside of the CaM regulatory and enzyme activity domains can determine the subcellular targeting of a particular CaM−enzyme complex, thereby contributing to the calcium signal transduction process through differential subcellular localization of the calcium signal transduction complex, and the calcium sensitivity and adaptability of the signal transduction complex can vary, depending on which particular CaM-regulated enzyme is in the complex with CaM. The approach described here can be extended to additional CaM-regulated enzymes and allow a more predictive approach to how eukaryotic cells

will respond to stimuli when the signal transduction response involves CaM-regulated pathways.

ACKNOWLEDGMENT

We thank Dr. Irving Klotz for stimulating discussions of the data and advice and Dr. Harvey Motulsky for providing a prerelease version of Prism 3.0. We are also grateful to Dr. Linda Van Eldik and Dr. Longyin Chen for their critical reading and comments on the manuscript.

REFERENCES

1. Nelson, M. R., and Chazin, W. J. (1998) in *Calmodulin and Signal Transduction* (Van Eldik, L. J., and Watterson, D. M., Eds.) pp 17−64, Academic Press, San Diego, CA.
2. Lukas, T. J., Mirzoeva, S., and Watterson, D. M. (1998) in *Calmodulin and Signal Transduction* (Van Eldik, L. J., and Watterson, D. M., Eds.) pp 66−168, Academic Press, San Diego, CA.
3. Van Eldik, L. J., and Watterson, D. M. (1998) in *Calmodulin and Signal Transduction* (Van Eldik, L. J., and Watterson, D. M., Eds.) pp 1−15, Academic Press, San Diego, CA.
4. Chin, D., and Means, A. R. (1996) *J. Biol. Chem. 271*, 30465−30471.
5. Chin, D., Sloan, D. J., Quiocho, F. A., and Means, A. R. (1997) *J. Biol. Chem. 272*, 5510−5513.
6. Zhang, M., Li, M., Wang, J. H., and Vogel, H. J. (1994) *J. Biol. Chem. 269*, 15546−15552.
7. Meyer, D. F., Mabuchi, Y., and Grabarek, Z. (1996) *J. Biol. Chem. 271*, 11284−11290.
8. Weber, P. C., Lukas, T. J., Craig, T. A., Wilson, E., King, M. M., Kwiatkowski, A. P., and Watterson, D. M. (1989) *Proteins: Struct., Funct., Genet. 6*, 70−85.
9. Craig, T. A., Watterson, D. M., Prendergast, F. G., Haiech, J., and Roberts, D. M. (1987) *J. Biol. Chem. 262*, 3278−3284.
10. Kosk-Kosicka, D., and Bzdega, T. (1991) *Biochemistry 30*, 65−70.
11. Gusev, N. B. (1995) *Biokhimiya (Moscow) 60*, 291−306.
12. Farrar, Y. J., Lukas, T. J., Craig, T. A., Watterson, D. M., and Carlson, G. M. (1993) *J. Biol. Chem. 268*, 4120−4125.
13. Shoemaker, M. O., Lau, W., Shattuck, R. L., Kwiatkowski, A. P., Matrisian, P. E., Guerra-Santos, L., Wilson, E., Lukas, T. J., Van Eldik, L. J., and Watterson, D. M. (1990) *J. Cell Biol. 111*, 1107−1125.
14. Harris, E., Watterson, D. M., and Thorner, J. (1994) *J. Cell Sci. 107*, 3235−3249.
15. Crivici, A., and Ikura, M. (1995) *Annu. Rev. Biophys. Biomol. Struct. 24*, 85−116.
16. Blumenthal, D. K., Takio, K., Edelman, A. M., Charbonneau, H., Titani, K., Walsh, K. A., and Krebs, E. G. (1985) *Proc. Natl. Acad. Sci. U.S.A. 82*, 3187−3191.
17. Lukas, T. J., Burgess, W. H., Prendergast, F. G., Lau, W., and Watterson, D. M. (1986) *Biochemistry 25*, 1458−1464.
18. Meador, W. E., Means, A. R., and Quiocho, F. A. (1992) *Science 257*, 1251−1255.
19. Haiech, J., Kilhoffer, M.-C., Lukas, T. J., Craig, T. A., Roberts, D. M., and Watterson, D. M. (1991) *J. Biol. Chem. 266*, 3427−3431.
20. Roth, S. M., Schneider, D. M., Strobel, L. A., VanBerkum, M. F. A., Means, A. R., and Wand, A. J. (1991) *Biochemistry 30*, 10078−10084.
21. Roth, S. M., Schneider, D. M., Strobel, L. A., Van Berkum, M. F. A., Means, A. R., and Wand, A. J. (1992) *Biochemistry 31*, 1443−1451.
22. Ehrhardt, M. R., Urbauer, J. L., and Wand, A. J. (1995) *Biochemistry 34*, 2731−2738.
23. Kilhoffer, M.-C., Kubina, M., Travers, F., and Haiech, J. (1992) *Biochemistry 31*, 8098−8106.
24. Gilli, R., Lafitte, D., Lopez, C., Kilhofer, M.-C., Makarov, A., Briand, C., and Haiech, J. (1998) *Biochemistry 37*, 5450−5456.
25. Sorensen, B. R., and Shea, M. A. (1998) *Biochemistry 37*, 4244−4253.
26. Shea, M. A., Verhoeven, A. S., and Pedigo, S. (1996) *Biochemistry 35*, 2943−2957.
27. Pedigo, S., and Shea, M. A. (1995) *Biochemistry 34*, 1179−1196.
28. Martin, S. R., Maune, J. F., Beckingham, K., and Bayley, P. M. (1992) *Eur. J. Biochem. 205*, 1107−1114.
29. Kilhoffer, M.-C., Roberts, D. M., Adibi, A., Watterson, D. M., and Haiech, J. (1989) *Biochemistry 28*, 6086−6092.
30. Protasevich, I., Ranjbar, B., Lobachov, V., Makarov, A., Gilli, R., Briand, C., Lafitte, D., and Haiech, J. (1997) *Biochemistry 36*, 2017−2024.
31. Watterson, D. M., and Vanaman, T. C. (1976) *Biochem. Biophys. Res. Commun. 73*, 40−46.
32. Perrin, D. D., and Sayce, I. G. (1967) *Talanta 14*, 833−842.
33. Martell, A. E., and Smith, R. M. (1974) *Critical Stability Constants*, Plenum, New York.
34. Womack, F. C., and Colowick, S. P. (1973) *Methods Enzymol. 27*, 464−471.
35. Klotz, I. M. (1985) *Q. Rev. Biophys. 18*, 227−259.
36. Stemmer, P. M., and Klee, C. B. (1994) *Biochemistry 33*, 6859−6866.
37. Hamlin, R. (1985) *Methods Enzymol. 114*, 416−452.
38. Howard, A. J., Nielsen, C., and Xuong, N. H. (1985) *Methods Enzymol. 114*, 452−472.
39. Brunger, A. T. (1992) *X-PLOR version 3.1. A system for X-ray crystallography and NMR*, Yale University Press, New Haven, CT.
40. Jones, T. A., Zou, J. Y., Cowan, S. W., and Kjeldgaard, M. (1991) *Acta Crystallogr. A47*, 110−119.
41. Jiang, J.-S., and Brunger, A. T. (1994) *J. Mol. Biol. 243*, 100−115.
42. Kleywegt, G. J., and Brunger, A. T. (1996) *Structure 4*, 897−904.
43. Luzzati, P. V. (1952) *Acta Crystallogr. 5*, 802−810.
44. Read, R. J. (1986) *Acta Crystallogr. A52*, 140−149.
45. Engh, R. A., and Huber, R. (1991) *Acta Crystallogr. A47*, 392−400.
46. Haiech, J., Kilhoffer, M.-C., Craig, T. A., Lukas, T. J., Wilson, E., Guerra-Santos, L., and Watterson, D. M. (1990) *Adv. Exp. Med. Biol. 269*, 43−56.
47. Haiech, J., Predeleanu, R., Watterson, D. M., Ladant, D., Bellalou, J., Ullmann, A., and Barzu, O. (1988) *J. Biol. Chem. 263*, 4259−4262.
48. Richards, F. M., and Vithayathil, P. J. (1959) *J. Biol. Chem. 234*, 1459−1465.
49. Török, K., Cowley, D. J., Brandmeier, B. D., Howell, S., Aitken, A., and Trentham, D. R. (1998) *Biochemistry 37*, 6188−6198.
50. Olwin, B. B., and Storm, D. R. (1985) *Biochemistry 24*, 8081−8086.
51. Klotz, I. M. (1997) *Ligand-receptor energetics: a guide for perplexed*, John Wiley, New York.
52. Meador, W. E., Means, A. R., and Quiocho, F. A. (1993) *Science 262*, 1718−1721.
53. Alber, T., Bell, J. A., Dao-Pin, S., Nicholson, H., Wozniak, J. A., Cook, S., and Matthews, B. W. (1988) *Science 239*, 631−635.
54. Matsumura, M., Becktel, W. J., and Matthews, B. W. (1988) *Nature 334*, 406−410.
55. Gross, D. S., and Garrard, W. T. (1988) *Annu. Rev. Biochem. 57*, 159−197.
56. Sternberg, M. J., Hayes, F. R., Russell, A. J., Thomas, P. G., and Fersht, A. R. (1987) *Nature 330*, 86−88.
57. Yuan, X., LiCata, V. J., and Allewell, N. M. (1996) *J. Biol. Chem. 271*, 1285−1294.
58. Hurley, J. H., Faber, H. R., Worthylake, D., Meadow, N. D., Roseman, S., Pettigrew, D. W., and Remington, S. J. (1993) *Science 259*, 673−677.
59. Goldsmith, E. J. (1996) *FASEB J. 10*, 702−708.
60. Koshland, D. E. (1998) *Nat. Med. 4*, 1112−1114.

BI9821263